Two-dimensional magnetic liquid froth: Coarsening and topological correlations

Florence Elias,[1] Cyrille Flament,[1] Jean-Claude Bacri,[1] Olivier Cardoso,[2] and François Graner[3]
[1]*Université de Paris 7 Denis Diderot, Unité de Formation et Recherche de Physique, Case 70.08, 2 place Jussieu, 75251 Paris Cedex 05, France*
*and Laboratoire d'Acoustique et d'Optique de la Matière Condensée, Case 78, 4 place Jussieu, 75251 Paris Cedex 05, France**
[2]*Laboratoire de Physique Statistique de l'Ecole Normale Supériure, 24 rue Lhomond, 75231 Paris Cedex 05, France†*
[3]*Laboratoire de Spectrométrie Physique, Université Joseph Fourier, Boîte Postale 87, 38042 Saint-Martin d'Hères Cedex, France‡*
(Received 2 December 1996)

We present an experimental study of a cellular system which may be formed in a two-dimensional (2D) layer made of an immiscible mixture of a magnetic fluid and an oil. We obtain a wet or a dry 2D froth, the characteristics of which are determined by the strength of an externally applied magnetic field. The froth is formed in an equilibrium state; the topological and geometrical features of the froth are fixed by the value of the applied field. The cellular pattern of the froth is stable in time, and a coarseninglike behavior is observed on decreasing the amplitude of the field. This cellular system can be used as a model to study topological processes in the equilibrium state, contrary to soap froths which are nonequilibrium systems because gas diffusion occurs. We show that the topological characteristics are statistically reversible after a magnetic-field cycle, and we present a statistical study of the froth features as a function of the amplitude of the field. The topological correlations between neighboring cells are well described by the Aboav-Weaire law. Finally, we consider the area of an n-sided cell, and show that its growth rate (magnetic field dependent) is, in a surprising manner, proportional to $n-6$, similarly to the Von Neumann law. [S1063-651X(97)10009-5]

PACS number(s): 82.70.Rr, 68.90.+g, 75.50.Mm

I. INTRODUCTION

A. Cellular patterns in physical systems

Cellular structures are observed in a wide variety of physical, biological, and ecological systems. They are a mass of domains (cells) made discrete by thin interfaces. The growth and statistical characterization of two-dimensional cellular structures has already been well studied [1–6]. In the case where a surface tension exists, the cellular structure presents an equilibrated pattern. Two-dimensional soap froths and magnetic garnet films are such well-studied systems. In this paper, magnetic liquid froths are considered and compared with these two cellular structures.

Soap froths are nonequilibrium systems. Since their energy includes solely the interfacial contribution, they coarsen in time in order to reach their final state, which corresponds to a minimal interface between air and water. During the coarsening process, the mean size of the soap bubbles increases and the number of bubbles decreases, with the result that the system becomes a single bubble [1–6]. It is possible to distinguish two phenomena which occur at very different velocities: a slow diffusion of gas between cells, and some topological reordering (a change in cell connectivity). Since the time scales of these phenomena are very different (of the order of several hours for the diffusion process and of the order of a second for the topological processes), the froth is usually considered as being in a quasiequilibrium state as regards the topological features.

Magnetic garnet films are completely different systems. When a magnetic field is applied perpendicularly to the film, a frothlike pattern is formed above a threshold value. The froth consists of bubbles which are domains of magnetization parallel to the field and a skeleton which is a domain of magnetization antiparallel to the field. This structure is stable in time but can be modified if the field is increased: all the magnetic dipoles tend to align along the applied field direction, with the result that the bubbles grow and the number of bubbles decreases. This evolution of the froth is called ''coarsening,'' in analogy to the evolution of the soap froths with time [7–11].

The changes in the properties of the two-dimensional froths during the coarsening process have been shown to obey some universal rules. The mechanical equilibrium at a vertex leads to the following feature: the number of edges impinging in a vertex is always equal to 3, and two edges at a vertex make an angle of 120°. Using Euler's theorem [2], and taking into account the previous observations, one deduces that the mean number of cell sides for an infinite system is equal to six. In the case of soap froths and bubble materials, the coarsening process shows a universal scaling state [4–6], during which the distribution function of the number of cell sides does not evolve, and the mean cell area follows a power law (as a function of time for the soap froth [4], and as a function of the applied field for the garnet film [7]).

B. Two-dimensional patterns in magnetic fluids

Our system is an immiscible mixture of an ionic magnetic fluid (MF) and an oil. The fluid is confined between two parallel plates and maintained in a horizontal position. Such

*LAOMC is associated with the CNRS (URA 800) and with the University Paris 6.

†LPS is associated with the CNRS (URA 1306) and with the Universities Paris 7 and Paris 6.

‡LSP is associated with the CNRS (UMR 5588).

a thin layer of MF, subjected to a vertical magnetic field, shows several patterns, a complete review of which is given elsewhere [12,13]. The parameters determining the properties of the froth are the amplitude of the magnetic field, H_{ext}, the volume fraction of MF, Φ, and the cell thickness h. If the magnetic field is static, it is possible to obtain either a labyrinthine pattern, consisting of the alternation of MF stripes and oil stripes intricated, or a bubble phase where MF bubbles surrounded by the oil form a hexagonal lattice. If the magnetic field is alternating, a froth phase is formed in which oil cells are surrounded by a skeleton made of MF. This latter phase is the dual conformation of the bubble phase.

All these patterns have the same energetic origin. A MF is a colloidal suspension of ferromagnetic particles, and each particle can be considered as a small magnetic dipole. The energy of the system contains two contributions: the interfacial MF-oil energy, and the magnetic energy. The latter can be split into two terms: the interactions between the magnetic dipoles and the external field, and the interactions among dipoles themselves. When a magnetic field is applied, all the magnetic dipoles align, and the average direction of each of the dipoles is parallel to the applied field. With the geometry described above, the magnetic dipoles repel each other, and thus tend to increase the interface between the oil and the MF. At the same time, the interfacial energy tends to minimize this interface, and, therefore, an equilibrium state is reached; the system forms the pattern with the lowest energy. Once the pattern is formed, it does not change with time. However, a coarsening of the froth phase can be obtained by decreasing the amplitude of the magnetic field. In this paper, we present a study of the evolution of the froth during the coarsening process. In particular, the statistical topological properties of the MF froth are shown to be reversible on cycling the magnetic field. We have verified that the shape of the cells are correlated and that these correlations are well described by the Aboav-Weaire relation [2,4,6]. This means that the number of sides of a cell is on average determined by the number of sides of the neighboring cells.

Let us note that Sudo, Hashimoto, and Katagiri [14] have studied an intermediate case between soap froths and magnetic liquid froths. Using a MF for which the MF-air surface tension has a very low value, they formed a two-dimensional (2D) soaplike froth by introducing bubbles of air in the MF, confined between two horizontal transparent plates. They showed that the application of a perpendicular magnetic field stabilizes the froth, but that the froth coarsens like a soap froth in the absence of a magnetic field. In the present work we focus on topological features of magnetic liquid froths in the equilibrium state (without diffusion). In soap froths the system is only in a quasiequilibrium state (because of diffusion). Consequently, in our work we differentiate the two effects.

II. EXPERIMENTAL SETUP AND FROTH FORMATION

We use an ionic MF (water based) with cobalt ferrite particles ($CoFe_2O_4$) with a mean size of roughly 10 nm [15]. This MF was synthesized by Neveu at the Laboratoire de Physico-Chimie Inorganique of the University Paris 6 following Massart's method [15]. The magnetic response of the

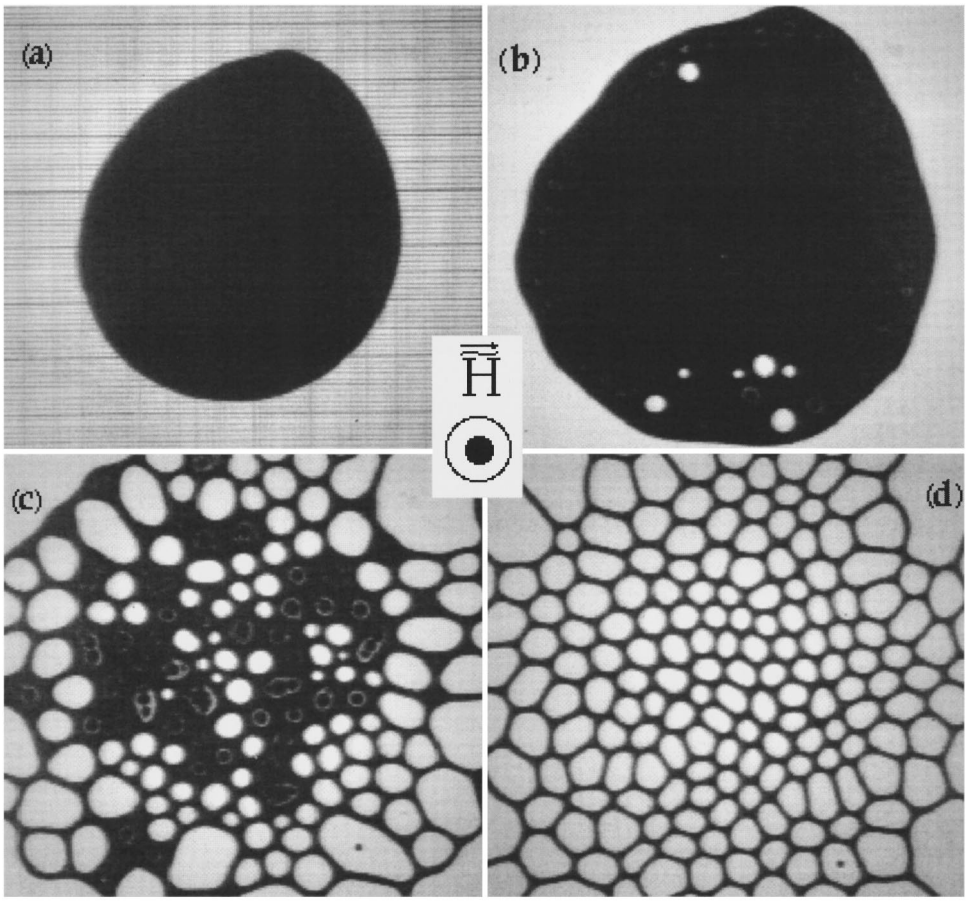

FIG. 1. Formation of a 2D magnetic liquid froth. A spatially homogeneous alternating magnetic field, $H = H_{ext}\cos(2\pi\nu t)$, is applied perpendicularly to the plane of the cell, $H_{ext} = 18.4$ kA m^{-1} and $\nu = 50$ Hz. (a) $t = 0$: in the initial situation a MF drop (in black) is surrounded by the immiscible liquid. (b) $t = 7$ min: several minutes after applying the magnetic field, some oil bubbles appear within the MF drop at the edges. (c) $t = 15$ min: the number of bubbles increases with time and the holes already formed at the edges grow. (d) $t = 97$ min: the equilibrium froth is formed. The scale is given by the underlying millimetric grid in the first photograph.

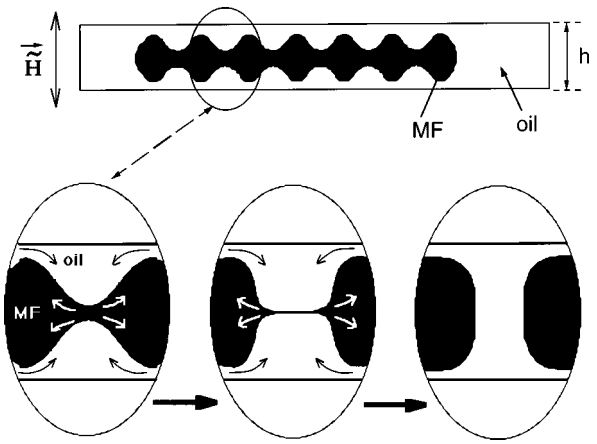

FIG. 2. Nucleation of an oil bubble within the MF. The applied alternating magnetic field generates an undulation of both interfaces between the oil and the MF at the top and bottom of the cell. The top sketch represents a transversal section of the cell in the initial state, corresponding to Fig. 1(a): the MF shape is circular when observed in a direction perpendicular to the cell, and the MF is surrounded by the oil. Below are sketched the stages of the oil hole formation. When the amplitude of the undulation is about half the cell thickness, h, the MF layer narrows locally. The dipole-dipole repulsions between the magnetic particles tend to increase this narrowing, and the oil flows over the MF in the region where the MF layer is a thin film. Finally, the film breaks and gives place to an oil hole.

MF is given by a Langevin-type law [16]. The MF saturation magnetization is $M_s = 40$ kA m^{-1}, and the susceptibility is $\chi \sim 1$ for low values of the field.

In the cell (thickness $h = 1$ mm), the MF is in contact with an immiscible organic liquid in order to avoid wetting phenomena. The MF does not wet the cell because a microscopic thin film of oil always lies between the MF and the cell walls. The value of the surface tension, σ, between the MF and the oil is determined *in situ* by measuring the critical wavelength at the threshold of the peak instability, or by measuring the deformation of a MF drop induced by an external magnetic field [17]: $\sigma \approx 10$ mN m^{-1} at room temperature. The magnitude of the surface tension does not depend on the amplitude of the magnetic field [17]. The effect of gravity is limited by reducing the density difference between the two fluids ($\rho_{MF} \approx 1600$ kg m^{-3} whereas $\rho_{oil} \approx 800$ kg m^{-3}). The cell is located between two coils in the Helmholtz configuration in order to have a spatially homogeneous magnetic field. The field alternates at a frequency, $\nu = 50$ Hz. The images are recorded by a CCD (couple charge device) camera and digitized by an acquisition card in a computer.

Photographs of the magnetic liquid froth formation are shown in Fig. 1. A single drop of MF surrounded by oil is shown in Fig. 1(a). On applying an alternating magnetic field at $t = 0$, bubbles of oil appear within the MF at the boundaries of the drop [Fig. 1(b)]. The number of oil bubbles increases with time as the bubbles already formed at the edges grow [Fig. 1(c)]. Figure 1(d) shows the equilibrium pattern. The formation time of the froth is of the order of several hours. Furthermore, the lower the amplitude of the magnetic field, the longer the froth formation time. The period of the field does not influence the froth formation, provided that it is longer than the Brownian rotation time of the magnetic particles (of the order of 1 ms [18]).

The nucleation of oil bubbles within the MF drop is due to a surface instability. Indeed, when subjected to an alternating field, a free horizontal interface of MF undulates. This effect is known as the Faraday instability [19]. As mentioned above, the MF and the cell walls are separated by a microscopic oil film. At the top and the bottom of the cell, both interfaces between oil and MF undulate (Fig. 2). When the amplitude of this undulation is about half the cell thickness, a hole of oil is nucleated in the MF drop. At the time of their initial appearance, all the oil holes have roughly the same diameter. Prior to the nucleation of the oil bubbles, the MF layer narrows and becomes a thin film. This film collapses and gives rise to an oil hole [Fig. 2, but regions in which a thin film of MF is present are also visible in Fig. 1(c)]. Note the importance of the thin oil film between the MF and the walls of the cell, within which the oil may flow to allow the nucleation of bubbles. As a result of this phenomenon, the magnetic liquid froth is not actually a 2D system, but only a quasi-2D system. Let us note that, once created, the froth remains stable if the alternating field is replaced by a static field.

III. GENERAL STUDY OF THE MAGNETIC LIQUID FROTH

The structure of the MF froth is quite different to the structure of the soap froth. In a two-dimensional soap froth, the liquid wets the walls of the cell. During the coarsening process, the bubbles grow or shrink because of gas diffusion through the soap film. Contrarily, the MF in a magnetic liquid froth is always separated from the transparent plates by a thin oil film. As a result, the structure formed by the MF is lacelike in character, that is, the two liquid phases are multiconnected. Boundary motions are possible because of the flow of oil between the MF and the cell walls.

Figure 3(a) shows a picture of so-called dry froth (in analogy with soap froths). Since the quantity of MF is small, the cells are faceted. In Fig. 3(c), the quantity of MF is greater and the oil bubbles are circular. Such a froth is called a ''wet froth.'' An intermediate case is shown in Fig. 3(b).

The structure of magnetic liquid froths conforms to some topological constraints, which govern all the two-dimensional cellular patterns, provided that the line tension has the same amplitude along the boundary. In particular, the number of edges impinging on a vertex always equals 3. Figure 4 shows the nonstability of a fourfold vertex. In this experiment, the formation of such a vertex is forced by introducing small pieces of soft iron above the cell. When a magnetic field is applied, the soft iron channels the field lines because of its high permeability, and generates local magnetic forces which attract the MF. One piece of soft iron is placed at the extremity of each of the four MF edges, and one above the fourfold vertex in order to stabilize it. When this latter piece is removed, the fourfold vertex becomes unstable and splits into two threefold vertices. This implies that threefold vertices are more energetically stable. These MF froths also confirm that individual cells have on average six sides, as predicted by Euler's theorem [1–6,20]. The angle between two boundaries impinging on a vertex is roughly

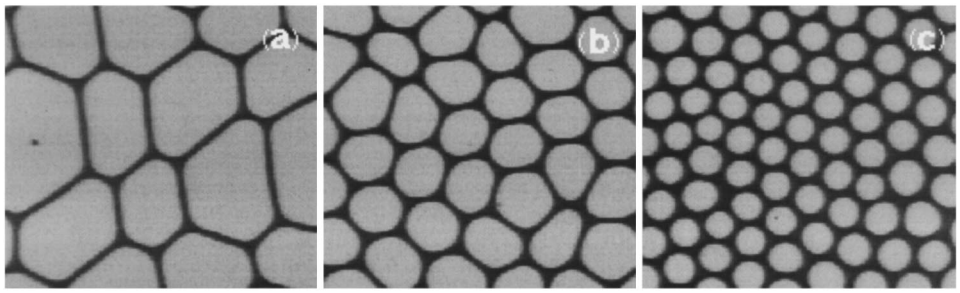

FIG. 3. Photographs of magnetic liquid froths obtained for three different values of the MF volume fraction: (a) $\Phi = 0.13$, (b) $\Phi = 0.21$, and (c) $\Phi = 0.35$. In (a) the froth is dry, meaning that the oil cells are faceted and separated by thin boundaries. Photograph (c) represents a wet froth: the cells are circular and the quantity of MF in the Plateau borders is important.

equal to 120° when the cells are faceted, as in Fig. 3(a) (this is one of Plateau's rules [1–3]). In this case, the edges of cells which do not have six sides are curved. They are, on average, convex if the cell has less than six sides, and concave if it has more than six sides.

A magnetic liquid froth coarsens on decreasing the amplitude of the magnetic field. The width of the MF boundaries is fixed by the amplitude of the external magnetic field, as in the stripe pattern [13]: the width increases when the field is decreased. Since the total quantity of MF is fixed, the total length of MF boundaries must then be decreased; therefore, some oil bubbles have to disappear. Two elementary transformations conserving the topological constraints are allowed. These transformations are known as $T1$ and $T2$ processes [2,3]. In a $T1$ process, an edge between two cells shrinks until it disappears, and another perpendicular edge is formed to avoid a fourfold vertex. The local connectivity of the cells involved in this process is changed with respect to the initial figure, and the number of sides is modified. In a $T2$ process, a cell shrinks and disappears, and its neighbors are rearranged in order to comply with the topological constraints. Figure 5 shows a $T1$ process observed in a magnetic liquid froth. The characteristic time of the boundary motion, when the amplitude of the magnetic field is changed, is of the order of a few seconds. We never observe a $T2$ process, probably because of the long-range repulsion between the MF boundaries. In fact, the process by which the bubbles increase their mean area in the MF froth, is coalescence (Fig. 6).

IV. STATISTICAL TOPOLOGICAL STUDIES OF THE COARSENING PROCESS

Here we present a statistical study of the evolution of the topological properties of the froth as a function of a decrease in the external field. We decreased the amplitude of the field step by step in small decrements, and waited for pattern equilibration between each step in order to observe a quasistatic phenomenon. The experiments were performed for three different values of the MF volume fraction Φ. The three corresponding froths are shown in Fig. 3.

Figure 7 shows the variation of the number of cells in the froth, as a function of the magnetic field. This curve must be read from right to left, because the froth is formed at a high value of the applied magnetic field, and then the field amplitude is decreased. Two regimes can be identified, regardless of the volume fraction of the MF. Above $9\ \mathrm{kA\,m^{-1}}$, the number of cells is constant, and no coalescence occurs. Nevertheless, some topological rearrangements ($T1$ processes) are observed. In order to understand this regime, we can only consider the magnetic fluid and modelize all the cell walls as one long stripe (we neglect here Plateau's borders). The width of this long stripe, e, is fixed by the strength of the field [13]. Consequently, within the framework of this approximation, the equilibrium state of the froth is reached when the cell boundary, that is, the long stripe, has a width equal to the equilibrium width: $e_0 = e(H_{\mathrm{ext}})$. Since the total area of the system is fixed, it is not always possible for the long stripe to reach its equilibrium value, and for

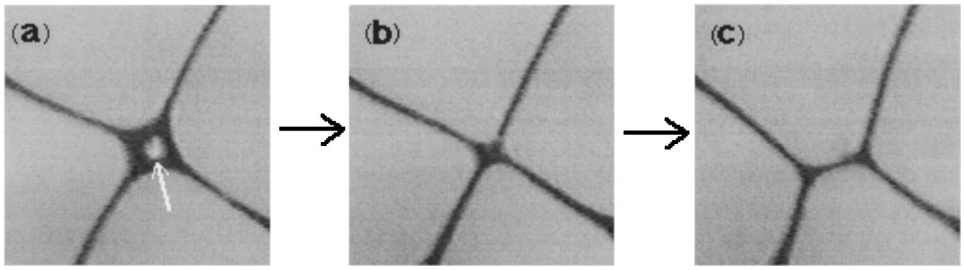

FIG. 4. Nonstability of a fourfold vertex. (a) shows the creation of a fourfold vertex which is forced by placing a small piece of soft iron at the vertex of a cell. This canalizes the field lines because of its high permeability, and thus generates local magnetic forces which attract the MF. At the edges and at the cross of the four MF branches, a piece of soft iron is present in order to fix them (a white circular piece is visible in the center of the first photograph). (b) was taken just after the piece of soft iron above the fourfold vertex was removed, and (c) several seconds later. The fourfold vertex spontaneously splits into two threefold vertices, which are more energetically stable for any values of the magnetic field.

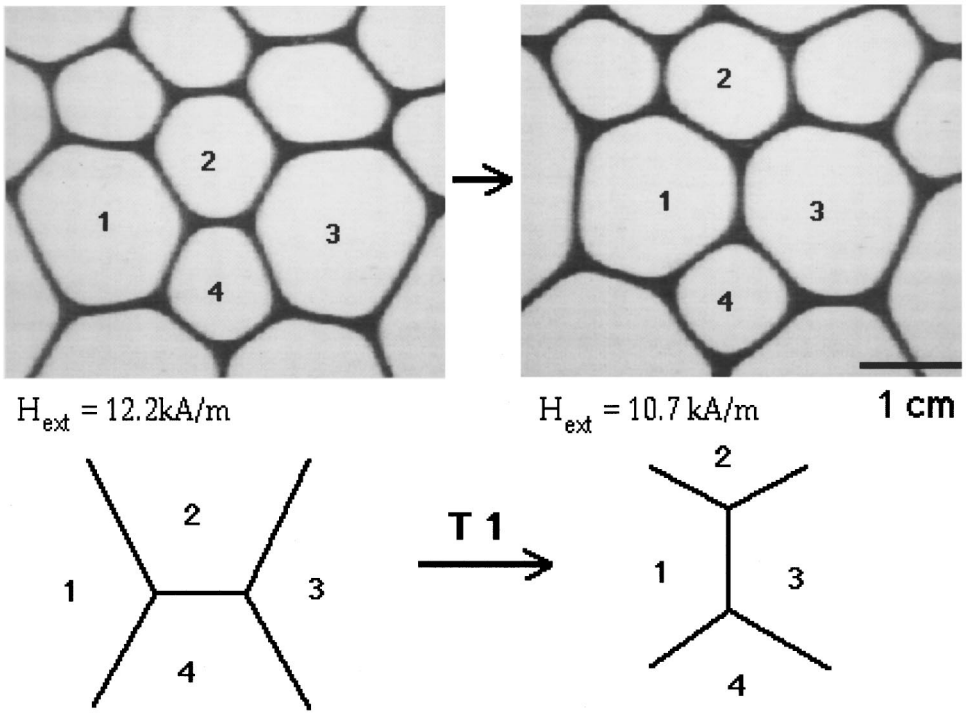

FIG. 5. A $T1$ process in a magnetic liquid froth. On decreasing the amplitude of the magnetic field, the edge between bubbles 2 and 4 disappears, and a new perpendicular edge is created between cells 1 and 3. The elementary process is sketched just below the photographs.

$H_{ext}>9$ kA m^{-1}, $e>e_0$. In reality, the thickness of the wall equals e_0, and the excess MF is localized in Plateau's borders: the vertices are MF reservoirs for the walls. On decreasing the field (to 9 kA m^{-1}) the wall thickness increases ($\partial e/\partial H_{ext}<0$), but the reservoirs play their role and reject a quantity of MF to the walls so that $e=e_0$. In other words, the system does not require cell destruction for the MF stripe to reach its equilibrium width: no cell is created or annihilated. We refer to this process ($H_{ext}>9$ kA m^{-1}) as regime I. Below 9 kA m^{-1}, cell coalescence is observed on decreasing the amplitude of the magnetic field. This process is the only means by which the cell edges acquire enough MF to increase their equilibrium width. We refer to this process as regime II ($H_{ext}<9$ kA m^{-1}).

Immediately following its formation, the froth is roughly monodisperse, meaning that the distribution function of the number of cell sides, $P(n)$, is narrow around its mean value which is 6. In the first regime of the coarsening process (above 9 kA m^{-1}), $P(n)$ is not affected by the $T1$ rearrangements. In fact, although the local connectivity of individual cells is modified by the $T1$ process, the statistical topological properties of the froth remain the same. In the second regime, $P(n)$ becomes extended and asymmetric (i.e., the third moment of the distribution is nonzero). The topological polydispersity of the froth is nevertheless somewhat poor. We observe cells with a number of sides, n, between 5 and 7, and occasionally 4, 8, or 9 sides. In comparison, the maximum value of n can be as large as 11 in 2D soap froths and magnetic garnet films. The evolution of $P(n)$ as a function of the magnetic field, does not seem to depend on the volume fraction of MF, Φ.

The coarsening of soap froths is time dependent and hence irreversible. The control parameter, that is, the magnetic field, which drives the evolution of magnetic liquid froths, is reversible. Hence it is possible to cycle the magnetic field in order to test the reversibility of the properties of the froth. Such an experiment is illustrated in Fig. 8. The photographs are the product of an image analysis. A homemade software program gives the skeleton of the froth, and assigns a color to each cell, depending on its number of sides

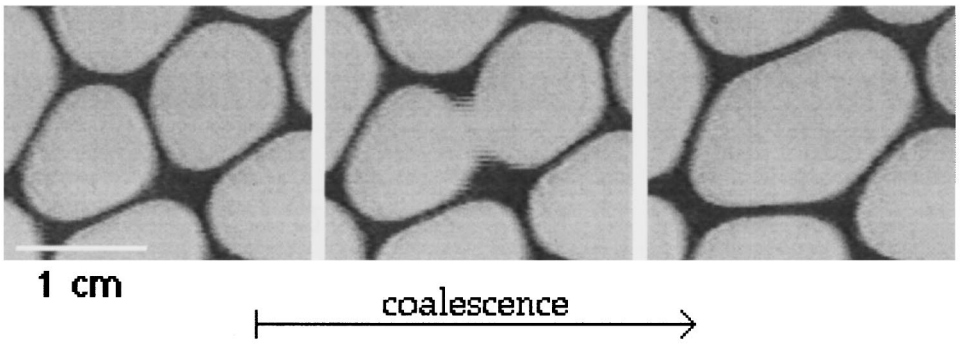

FIG. 6. Break of an edge between two cells. This is the mechanism by which the cells disappear in a MF froth when the magnetic field is decreased. Starting from an initial froth, the amplitude of the field is then decreased. The photographs represent, respectively, the situation prior to, during, and immediately after the wall destruction. The characteristic time of this process is of the order of a second.

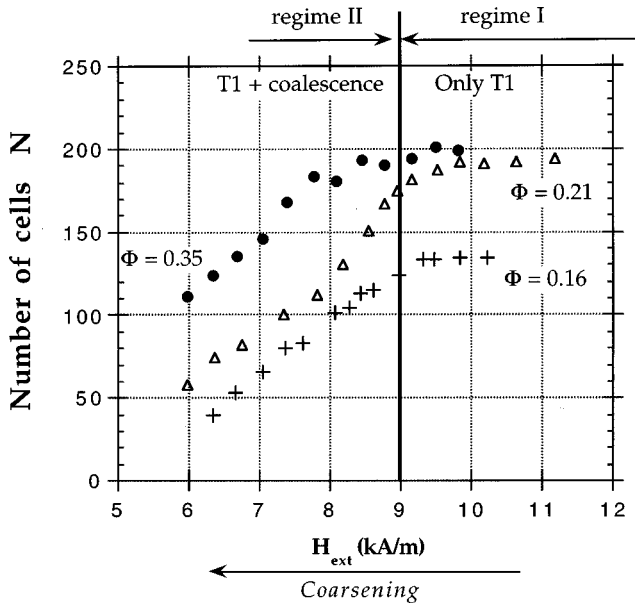

FIG. 7. Evolution of the number of cells N during the coarsening process for three different values of the MF volume fraction Φ. This graph must be read from right (high amplitudes of the external field) to left (low values), because the coarsening process occurs as the magnetic field is decreased. Two stages are clearly apparent, regardless to the value of Φ. For $H_{\mathrm{ext}}>9\ \mathrm{kA\ m^{-1}}$ (regime I), N remains constant, meaning that no cell disappears, thus the froth evolution is driven by the $T1$ processes. For $H_{\mathrm{ext}}<9\ \mathrm{kA\ m^{-1}}$ (regime II), oil bubbles coalesce together so N decreases, while $T1$ rearrangements are still observed.

[21]. The froth is created at an initial value of the magnetic field in regime I, $H_1=10.3\ \mathrm{kA\ m^{-1}}$, and then the field is decreased to regime II. The total number of cells decreasessome seven-sided cells appear, and the number of five-sided , cells grows. When the amplitude of the field is increased to its initial value, no new cell is created, but the seven-sided cells disappear and the number of five-sided cells is reduced. The distribution function is the same before and after one cycle, but does change during the cycle. This means that the topological statistical properties of the froth are reversible, although the geometrical properties of the froth (for instance, the mean cell area) are not reversible within a magnetic-field cycle.

V. TOPOLOGICAL CORRELATIONS

Here we present some results concerning cell shape correlations between neighboring bubbles. The results are considered in the light of the Aboav-Weaire law [2,4,6] which linearly links the mean number of edges of the first neighboring cells of an n-sided cell, $m(n)$, with $1/n$:

$$m(n)=6-a+\frac{6a+\mu_2}{n}, \tag{1}$$

where μ_2 is the second-order moment of the distribution, $P(n)$, of the number n of cell edges, and a, an empirical parameter. A simpler equation may be derived by introducing the notion of a ''topological charge'' [4], $\tau=n-6$. As a consequence of Euler's law, $\langle\tau\rangle=0$ for an infinite system. Let us consider a fluctuation τ_0 of this charge, i.e., a cell with a number of sides $n=6+\tau_0$. If this fluctuation is locally resorbed, the topological charge, τ_0 has to be distributed over the nearest neighbors. Hence the average topological charge of the n nearest neighbors is $-\tau_0/n=6/n-1$. Then the mean number of edges of the neighboring cells is $m(n)=6+(-\tau_0/n)=5+6/n$. This is Eq. (1) for the particular

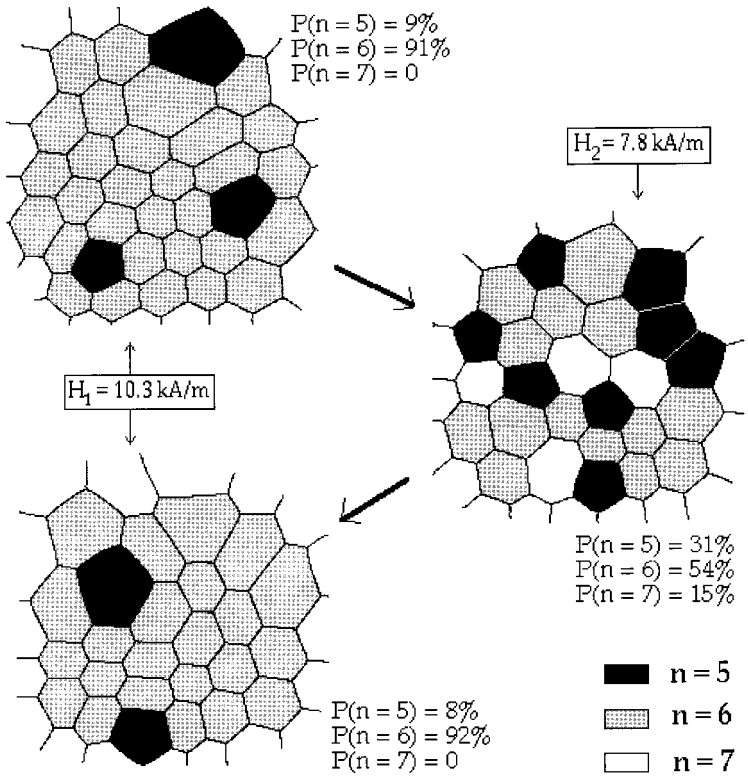

FIG. 8. Reversibility of the statistical topological properties of the froth. Skeletons of the froth during a cycle are represented. The magnetic field is decreased to $7.8\ \mathrm{kA\ m^{-1}}$ (in regime II), the amplitude of which initially equals to $10.3\ \mathrm{kA\ m^{-1}}$ (in regime I), and then increased to its initial value. At low field, the total number of cells is lower than in the initial state, and the disorder is greater. In the final state, the total number of cells is lower than in the initial state, but the disorder is the same. The values of the distribution function of cell sides are reported for each configuration.

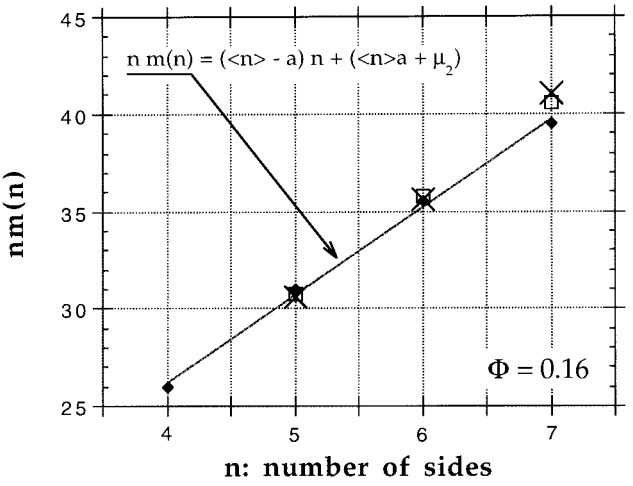

FIG. 9. Curve of the product $nm(n)$ vs n for $\Phi=0.16$ and for different values of the magnetic field. We also indicate between brackets the value of the average number of sides and the second-order moment of the side distribution for a given field. With a black lozenge icon$\rightarrow H_{ext}=6.3$ kA m^{-1} ($\langle n\rangle=5.80$ and $\mu_2=0.42$), cross icon$\rightarrow H_{ext}=8.6$ kA m^{-1} ($\langle n\rangle=5.91$ and $\mu_2=0.22$) and square icon$\rightarrow H_{ext}=10.3$ kA m^{-1} ($\langle n\rangle=5.95$ and $\mu_2=0.14$). We obtain $a\approx 1.0$ for $\Phi=0.16$ and for all values of the applied field.

values $a=1$, $\mu_2=0$, and this condition corresponds to a screening of the charge τ by the cell nearest neighbors. Consequently, the main feature is that ''anticorrelations'' exist between a cell and its nearest neighbors, i.e., a cell with a large number of sides (typically $n>6$) is surrounded automatically by cells with a few sides ($n<6$), and *vice versa* [22].

The quantity $m(n)$ is directly computed by our home-made software [21]. We performed measurements for a dry froth and a wet froth (actually the number of edges is the number of neighboring cells) and for different values of the applied field. We used a modified formulation of Eq. (1), since our system contains a finite number of cells (i.e., $\langle n\rangle$ does not exactly equal 6 [20]), which depends on H_{ext}: $nm(n)=[\langle n(H_{ext})\rangle-a)n+(\langle n(H_{ext})\rangle a+\mu_2(H_{ext})]$. The results for a dry froth are presented in Fig. 9, where the quantity $nm(n)$ versus n is plotted. In all cases (wet and dry), the Aboav-Weaire law is applicable. The value of the empirical parameter a depends on the surface fraction Φ, but does not depend on the strength of the magnetic field. The value of a is determined using a least-squares method, for instance, $a=1.00$ for $\Phi=0.13$ and $a=1.17$ for $\Phi=0.35$, for $H_{ext}=6$ to 11 kA m^{-1}. These values are very close to those typically obtained in the soap froths ($a=1$) [4], and in the garnet film experiments ($a=1.2$ for a high magnetic field, and $a=1.5$ in zero field) [7]. It appears that the value of a seems to depend only on the cell topology, despite the fact that the cell interaction mechanisms in these various physical systems are completely different [23].

It is also possible to visualize the screening of the topological charge by the presence of clusters made of several cells with $n\neq 6$. Starting with an ordered hexagonal pattern and decreasing H_{ext}, we observe the transformation of two neighboring six-sided cells into two n-sided cells (with $n_1<6$ and $n_2>6$) by $T1$ process(es). This is illustrated in Fig. 10 by the presence of cell pairs ($n_1=5$, $n_2=7$). We note that,

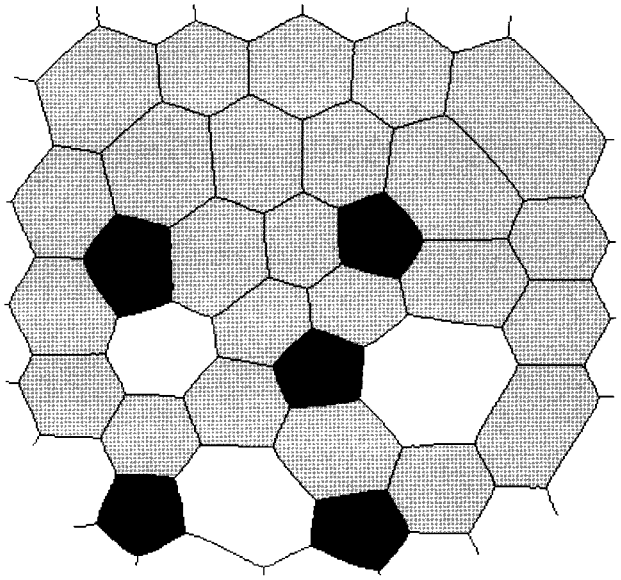

FIG. 10. Framework of a dry froth ($\Phi=0.16$) for $H_{ext}=8.6$ k A m^{-1} with a singleton ($n=5$), two doublets ($n=5$ and 7), and a triplet ($n=5$, 7, and 5).

for high values of the magnetic field, the topological changes occur mainly at the boundary of the system. For low values of H_{ext}, we also observe the nucleation of these clusters in the center of the experimental cell. The lower the field, the higher the number of cells inside a cluster.

VI. GEOMETRICAL STUDIES

In this last section we present some measurements of the cells' area. First, we focus on the average area of the cells as a function of the external field H_{ext}. Second, we consider the area of an n-sided cell as a function of H_{ext} and n.

The variation of the mean cell area, $\langle A\rangle$, as a function of the external field for different surface fractions ($\Phi=0.16$, 0.21, and 0.35) is plotted in Fig. 11. For the dry froths ($\Phi=0.16$ and 0.21), three regimes are evident. For high values of the magnetic field (from 11 to 9 kA m^{-1}, that is, in regime I), $\langle A\rangle$ is constant. During regime I, only $T1$ processes occur; therefore, the number of cells remains constant (see Fig. 7). Since no cell is created or destroyed, the average area $\langle A\rangle$ remains constant.

From $H_{ext}=9$–7 kA m^{-1} (regime II), $T1$ processes, and also cell coalescence, occur. Consequently, the average cell area increases. Cell coalescence occurs because the quantity of MF needed to satisfy the condition $e_0=e(H_{ext})$ is not present in Plateau's borders (see Sec. IV). We can establish the scaling behavior of $\langle A\rangle$ with H_{ext} as follows. Neglecting Plateau's border, the total area occupied by the MF is determined by the surface of the cell walls, $S_{MF}\cong Ne\sqrt{\langle A\rangle}$, where e is the thickness of the edges. The total area of the system is $S_{total}=S_{MF}+N\langle A\rangle$, which is related to the surface fraction by $S_{total}=S_{MF}/\Phi$. Thus we obtain the average area of a cell, $\langle A\rangle$, as a function of e and Φ. Postulating a simplified, but realistic law of variation of e with the applied field. $e\approx 1/H_{ext}$ [24], we obtain the following scaling behavior $\langle A\rangle\approx 1/H_{ext}^2$. The measured values of the average cell area correlate quite well this prediction, as illustrated in Fig. 11.

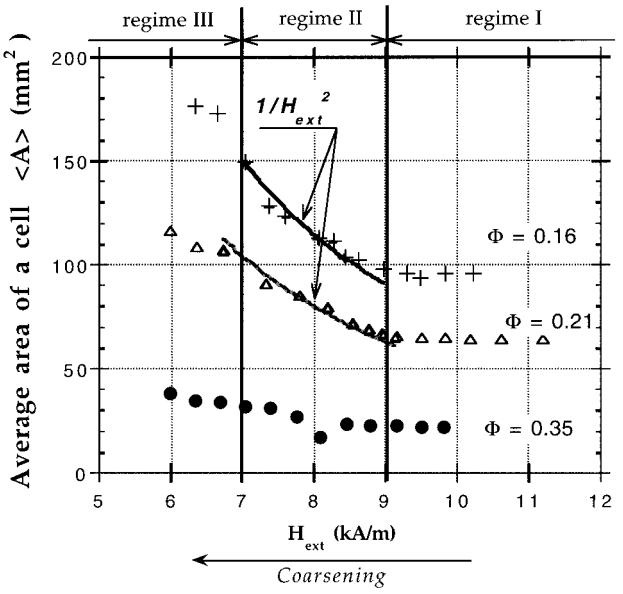

FIG. 11. Mean area of the cells $\langle A \rangle$ plotted as a function of H_{ext} for $\Phi = 0.16$ (cross icon; dry froth), $\Phi = 0.21$ (triangle icon), $\Phi = 0.35$ (black circle icon; wet froth). The limits of the three regimes (see text) are defined by two vertical lines. In regime II the data are fitted by $\langle A \rangle \cong 1/H_{\text{ext}}^2$ for $\Phi = 0.16$ and 0.21.

For the lowest values of the external field, $H_{\text{ext}} < 7$ kA m^{-1} (regime III), the global froth is free, that is, the froth does not touch the boundaries of the cell, and, consequently, Φ increases. We can also note that for the wet froth ($\Phi = 0.35$), $\langle A \rangle$ is roughly constant.

We also measured the area of an n-sided cell (without statistical averaging) as a function of the external field in regimes I and II. In Fig. 12 the cell area A_n is plotted as a function of the magnetic field, for different cell side numbers, $n = 5$, 6, and 7. These measurements were made on the dry froth for which $\Phi = 0.13$. The obvious conclusions are as follows: in regime I, for $n = 6$ (i.e., $\tau = 0$), A_6 remains constant; for $n = 5$ ($\tau = -1$), A_5 increases when the magnetic field decreases; and for $n = 7$ ($\tau = 1$), A_7 decreases when the field decreases. It is interesting to note that the cell area seems to vary linearly with the field, and that the slope of A_5 as a function of field is roughly the opposite of A_7. These observations lead us to postulate a growth rate with the magnetic field, proportional to the topological charge $\partial A_n / \partial H_{\text{ext}} \approx (n-6)$, in a manner similar to the Von Neumann prediction for the time growth rate of 2D soap bubbles [2,3]. In regime II, the area of n-sided cells remains roughly constant until coalescence occurs, which gives rise to a sudden increase in the area of the cell and the average area of the cells.

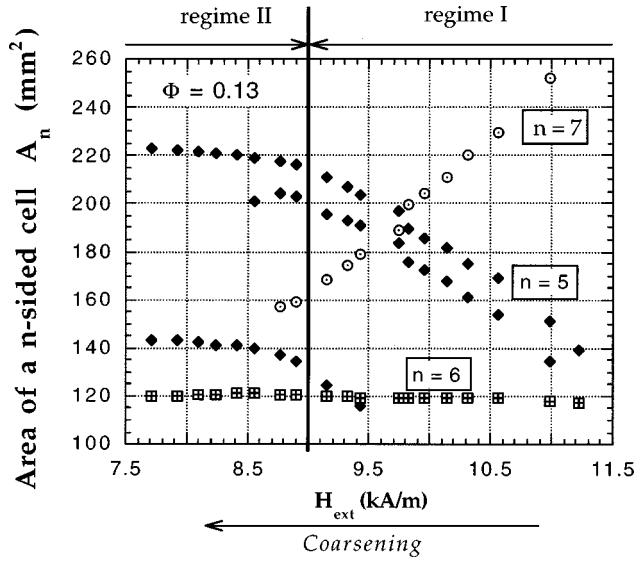

FIG. 12. A_n plotted as a function of the external magnetic field in regime I (where only $T1$ processes occur) for $n = 5$, 6, and 7. The growth rate of an n-sided cell with the external field follows a quasi-Von Neumann law. In regime II (with $T1$ and coalescence between cells), A_n remains constant for all values of n and H_{ext}.

VII. DISCUSSIONS AND CONCLUSIONS

To summarize, we present a two-dimensional cellular system with characteristics intermediate between those of soap froths and magnetic garnet films. The topological and the geometrical characteristics of the system are determined by the value of the applied magnetic-field strength, and do not coarsen in time since an equilibrium state is reached. However, a coarseninglike process can be induced by decreasing the amplitude of the external field. Since time is not a relevant dimension in this system, the coarsening process can be reversed. In fact, we have shown that the topological statistical characteristics are reversible after a magnetic-field cycle. This means that the coarsening of the magnetic liquid froth can be reversed, contrary to the soap froths, for which the evolution is irreversible. The area of an individual n-sided cell is proportional to its topological charge $n-6$, and varies linearly with the external field. This quasi-Von Neumann law (our so-called growth rate represents the variation of the cell area with the applied field instead of time) is valid in regime I, where only $T1$ processes occur. In this regime, the average area of the cells remains constant. When cell coalescence occurs (regime II), the area of an n-sided cell remains constant (for any value of n) until coalescence with another cell occurs. Consequently, the average area of the cells increases. An additional local study on a single bubble is required to better understand this Von Neumann behavior. The question is whether an effective Laplace law (including magnetic phenomena) can be formulated in this case.

The observed macroscopic cellular pattern can be employed for topological studies because the magnetic liquid froth is in an equilibrium state for a given value of the external field. In a soap froth, gaseous diffusion is superimposed on the topological processes, meaning that the froth is only in a quasiequilibrium state. In the garnet systems it is not possible to observe directly a topological rearrangement because it occurs very quickly (even with a speed video camera it is not possible to visualize a $T1$ process). Our system can be effectively used as a model system to differentiate the diffusion effect and the topological changes. Furthermore, the 2D magnetic liquid froth presents an advantage in that the vertices may be pinned by a local magnetic force (as described in the text), and consequently the topology is forced. For instance, it is possible to create a defect in an

equilibrated froth, and study the relaxation toward equilibrium. Such experiments should allow us to determine the exact role played by the topological $T1$ processes. This system is the only one where vertices can be manipulated; in garnet systems only collapses can be induced [25]. One inconvenience of this cellular system is that the number of cells is relatively small. Consequently, the statistics are poorer than those obtained in an equivalent soap froth study. Additionally, the distribution of the number of cell sides is not very broad; nevertheless, it permits an easy visualization of the screening of the topological charge. This experimental study will be completed in a further work by a theoretical treatment of the geometrical data and a description of a conformational instability (bending instability of the MF walls between the cells) which occurs for high values of the magnetic field [12].

ACKNOWLEDGMENTS

We would like to thank Pierre Mohlo, Stephane Douady, and Eytan Domany for fruitful discussions, Sophie Neveu for providing us with the magnetic fluid, and Patrick Lepert and Jacques Servais for constructing the experimental device.

[1] D. Weaire and N. Rivier, Contemp. Phys. **25**, 59 (1984).
[2] J. Stavans, Rep. Prog. Phys. **56**, 733 (1993).
[3] J. A. Glazier and D. Weaire, J. Phys. Condens. Matter **4**, 1867 (1992).
[4] J. Stavans and J. A. Glazier, Phys. Rev. Lett. **62**, 1318 (1989).
[5] J. A. Glazier, Ph.D. dissertation, University of Chicago, 1989 (unpublished).
[6] B. Levitan and E. Domany, Int. J. Mod. Phys. B **10**, 37 (1996).
[7] K. L. Babcock, R. Seshadri, and R. M. Westervelt, Phys. Rev. A **41**, 1952 (1990).
[8] K. L. Babcock and R. M. Westervelt, Phys. Rev. A **40**, 2022 (1990).
[9] K. L. Babcock and R. M. Westervelt, Phys. Rev. Lett. **63**, 175 (1989).
[10] D. Weaire, F. Bolton, P. Molho, and J. A. Glazier, J. Phys. Condens. Matter **3**, 2101 (1991).
[11] M. Portes de Albuquerque and P. Mohlo, J. Magn. Magn. Mater. **113**, 132 (1992).
[12] F. Elias, C. Flament, J. C. Bacri, and S. Neveu, J. Phys. I **7**, 711 (1995).
[13] C. Flament, J.-C. Bacri, A. Cebers, F. Elias, and R. Perzynski, Europhys. Lett. **34**, 225 (1996).
[14] S. Sudo, H. Hashimoto, and K. Katagiri, J. Magn. Magn. Mater. **85**, 159 (1990).
[15] S. Neveu-Prin, F. A. Tourinho, J.-C. Bacri, and R. Perzynski, Colloids Surf. A **80**, 1 (1993).
[16] R. E. Rosensweig, *Ferrohydrodynamics* (Cambridge University Press, Cambridge, 1985).
[17] C. Flament, S. Lacis, J.-C. Bacri, A. Cebers, S. Neveu, and R. Perzynski, Phys. Rev. E **53**, 4801 (1996).
[18] J.-C. Bacri, J. Dumas, D. Gorse, R. Perzynski, and D. Salin, J. Phys. (France) Lett. **46**, L1199 (1985).
[19] J.-C. Bacri, A. Cebers, J.-C. Dabadie, S. Neveu, and R. Perzynski, Europhys. Lett. **27**, 437 (1994).
[20] The mean value of the number of sides of the cells, $\langle n \rangle$, is in fact less than 6, because of the finite size of our experimental system (the Euler theorem is established for an infinite two-dimensional Euclidean space). $\langle n \rangle$ is generally about 5.95 at the beginning of the experiment, when the number of cells is maximum, and decreases toward 5.6 to 5.8 at the end of the coarsening process, because the statistics are measured on less than ten cells.
[21] This home-made software program consists of a user module for NIH Image by Wayne Rasband, National Institutes of Health. Both source code and compiled application for Mac OS are available at http://www.lps.ens.fr/~cardoso/
[22] An empirical relation for the mean area of an n-sided cell is given by the Lewis law: $x_n = b + \lambda(n-6)$, where $x_n = \langle A_n \rangle / \langle A \rangle$, b and λ are pattern-dependant constants [1,23]. Here again, the mean area is proportional to the topological charge $\tau = n - 6$. Consequently, the average area of the cells with $n < 6$ is less than that of the cells with $n > 6$, and, furthermore, as a consequence of the Aboav-Weaire law, the smaller cells are surrounded by larger cells (i.e., $n > 6$). This fact is a crucial property of the cellular patterns.
[23] M. Seul, N. Y. Morgan, and C. Sire, Phys. Rev. Lett. **73**, 2284 (1994).
[24] A complete calculation for parallel infinite stripes [13] gives the period of the stripe pattern as a function of the external field. Using a truncated formula we get $\sigma h / l^2 \approx [(\mu_0 M^2 / 4\pi) \sin(\pi\Phi)/\pi^2]$. With $\Phi = (e/l) = \text{const}$, and $M = \chi H_{\text{ext}}$, we obtain $e \cong 1/H_{\text{ext}}$.
[25] P. Mohlo (private communication).